

# Shock Tube Literature Final Design Report

Alexander Ephraim\*, Eric Yoerg† Kassandra Durst‡, Kalista Curtis§, and Mason Dunsmuir¶  
*Embry-Riddle Aeronautical University, Daytona Beach, Florida, 32114*

## I. Nomenclature

$M_s$	=	Incident shock mach number
$p_4$	=	driver pressure
$p_1$	=	driven section pressure
$\gamma_1$	=	driven section ratio of specific heats
$\gamma_4$	=	driver section ratio of specific heats
$a_1$	=	driver speed of sound
$a_2$	=	driven section speed of sound

## II. Introduction and Purpose

**S**HOCK tubes are invaluable research tools in fluid dynamics, offering a controlled environment for studying high-speed flow phenomena such as shock waves, detonations, and boundary layer interactions. The primary objective of this effort was to design and construct (or refurbish) a shock tube facility that would provide students with a hands-on learning experience in experimental fluid dynamics. This facility should enable students to conduct experiments, collect data, and analyze the results, thereby enhancing their understanding of compressible flow and its applications. This report documents the initial project design requirements, details of the design and analysis, testing and results, and lastly, lessons learned and recommended next steps.

## III. Design

### A. Capability Gap

The AE315 laboratory lacked a shock tube facility. Shock tubes are relatively inexpensive and generate 1D, unsteady flows, easily comparable to theory learned in class. Depending on the initiation mechanism and design pressure, they can also be very simple to assemble and operate. The compressible flow portion of the experimental aerodynamics lab was already very limited; thus, a shock tube was a ideal candidate for expanding the scope of labs for the aforementioned reasons.

### B. Original Technical Objectives

Below is a list of the original technical objectives which were set by the design team in the proposal. They are a response to the RFP from Dr. Surabhi Singh which simply required a "basic shock tube" to be used by students. Additional tasks, categorized as "if time allows" included a test-section for visualization, additional surface pressure ports, and pressure transducers. Pressure transducers and an accompanying signal conditioner were excluded from this list initially due to budgetary limits; however, a custom adapter was designed and materials purchased to allow PCB ICP dynamic pressure transducers to be integrated into the assembly in the future.

- 1) Goal: Design a test-section which provides optical access for schlieren imaging as well as future uses in impulse testing of PSP (Visible back wall). FEA analysis will be conducted to verify the structural integrity of the design to an agreed on F.O.S. with the aerospace engineering department.

---

\*Graduate Researcher, Aerospace Engineering

†Graduate Researcher, Aerospace Engineering

‡Undergraduate Researcher, Aerospace Engineering

§Undergraduate Student, Aerospace Engineering

¶Undergraduate Student, Aerospace Engineering

- 2) Design new or outfit existing piping assembly with appropriate fittings, gaskets, and bolts to maintain a proper seal at the expected maximum pressures.
- 3) Design a fusing circuit or calibrate diaphragms to initiate the shock tube.
- 4) Design a stand to secure the shock tube horizontally
- 5) Author SOP outlining the steps required to operate the facility and safety considerations. This should be refined into a final copy at the end of the project to be used for students and TA.
- 6) Assemble the shock tube and integrate the shock tube and fusing circuit
- 7) Test the shock tube and characterize the flow using schlieren imaging
- 8) Design a potential experiment for AE315 Lab using the new shock tube

All technical objectives were met with the exception of a complete AE315 experiment and an EHS approved SOP. Due to primarily issues with lead times, an unknown budget, and delays in the design process, key components such as the test-section and timing transducers were not delivered by the due date for the final report. Only after instrumentation and a test-section is integrated into the facility and tested will a final SOP be written. Once an SOP is changed it must be re approved by EHS; thus, it is preferable to have a complete facility before approval for students to use. However, a draft SOP, covering the testing procedure, and a potential experiment was created to begin this process.

### C. Trade Study: refurbish vs new design

The most significant decision that was made during the design process was whether to build a completely new shock tube or refurbish an existing facility. The primary factors which influenced this decision included safety, budget, and project scope. The design(s) for a newer, larger shock tube facility required professional welding work on stainless steel by a certified/licensed welder for the facility to be considered safe. The material costs without manufacturing was below the given range; however, welding work was found to be exceedingly expensive for the larger joints, nearly doubling the total price. Ultimately the decision was made to refurbish the existing 2 in internal diameter shock tube as this option allowed the project to remain within a reasonable budget while fulfilling all initial project requirements as well the addition of a test-section and pressure sensing ports. Additionally, all existing piping and connections conformed to ASME standards; thus, no additional analysis was required for piping and instrumentation to consider the facility safe under specific design conditions.

### D. Final Design Overview

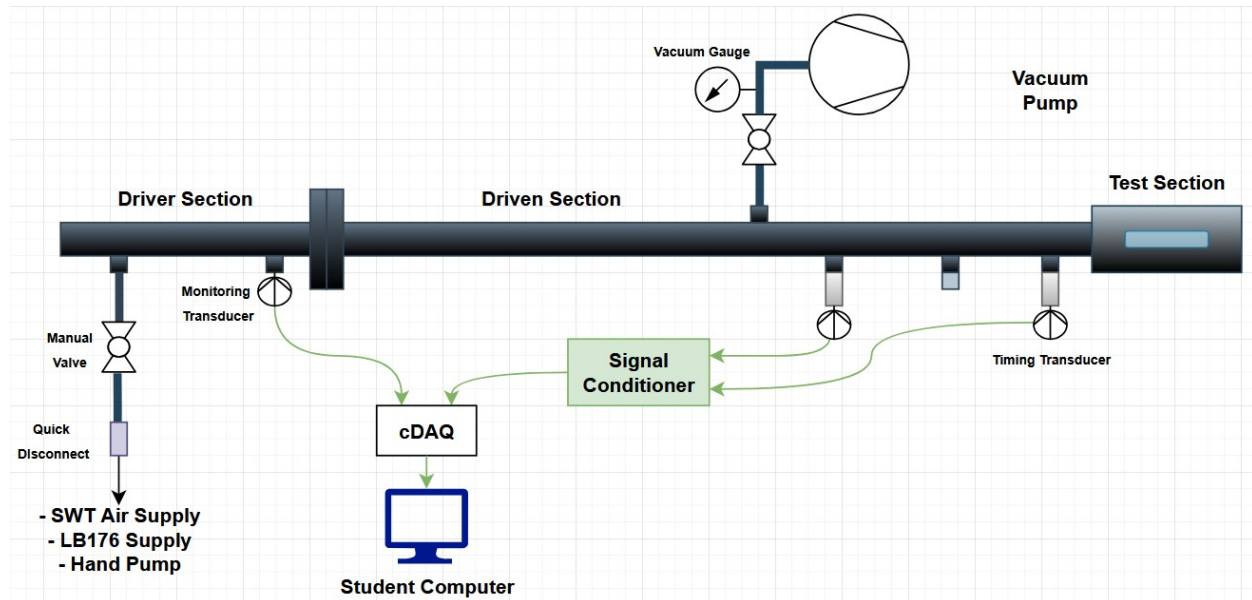


**Fig. 1 Schematic of Final Design**

Figure 1 details the completed facility as it will be used for AE315 lab. The shock tube is constructed out of 2 in NPS Schedule 80 304/304L Stainless Steel pipe. The driver section and driven section are connected by Class 300

316/316L Stainless Steel raised face NPT threaded flanges. Two full face Garlock Blue Guard 3000 Gaskets seal the flange connection and secure the mylar diaphragms, separating the driver and driven sections. The flange connection is bolted per Garlock's Gasketing Technical Manual using eight ASTM A913 B7 5/8 - 11 bolts and accompanying F436 washers, and A194 2H nuts. Each bolt is lubricated using Loctite LB8150 anti-seize to reduce preload scatter and torqued to 80 ft-lbs using a calibrated torque wrench, per the assembly instructions of Garlock's manual. All other connections directly to the shock tube are accomplished using six 1/4 NPT weld on buns.

The driver section is closed on one end using a threaded cap. Two 1/4 NPT ports are available, one of which houses an analog pressure transducer which measures from 0 to 200 psig at 1kHz. The other port includes a pipe nipple, followed by a manual inline valve, and a female industrial quick disconnect. The shock tube may be supplied air using the wall pressure regulator in LB176 (up to 80 psig) or the SWT pressure regulator (up to 160 psig) in LB182. Air is supplied through an air hose, which connects to the LB176 regulator directly with a 1/4 NPT fitting or to the SWT regulator using a female 1/4 NPT to male 2 NPT adapter. To trigger the shock tube, sufficient pressure to burst the diaphragm is supplied through the hose and the manual inline valve is opened to slowly increase the pressure until burst.

The driven section is 8 ft long and can be capped on one end with a threaded pipe cap or the test-section. Additionally, it may be configured with an open end to capture free expansion of the shock wave, as in the case of testing described in this report. Four 1/4 NPT ports, equally spaced 1 ft apart near the end are available. Two will house dynamic pressure transducers for measuring the shock wave pressure profile and timing the optical diagnostics by measuring the time of arrival and thus shock velocity before reaching the test-section. Specialized adapters, explained in a later section, were designed to flush mount the transducers into the wall of the pipe. A third port is available to vacuum the driven section to reach higher pressure ratios. A pipe nipple connects to a manual inline valve, followed by a two female x one male 1/4 NPT tee. A vacuum gauge (30 - 0 inHg) occupies one female port and an 1/4 male NPT to 1/2 SAE adapter occupies the other. A vacuum pump supplied by the LB182 can attach directly to this adapter. A fourth port is available for repositioning of the timing transducers or for additional sensors in the future. Ports that are not in use are plugged.

Piping Component	Maximum Pressure (psig)	Source
Blue Guard 3000 Gaskets, Class 300 Flanges	800 (reliable seal)	Manufacturer
1/4" NPT SS Bungs	2500	ASME B16.11
Schedule 80 2 in NPS Pipe	1985	ASME B31.1
Schedule 40 2 in NPT Pipe Cap	1000	ASTM A182
1/4 NPT Male x1 1/4 NPT Female x2 Vacuum Tee	1000	Manufacturer
1/4 NPT Vacuum Gauge	not reported	Manufacturer
25 ft 1/4 NPT hose	200	Manufacturer
Dixon F2D2-S Quick disconnect male	500	Manufacturer
Dixon 2FM2 Quick disconnect female	500	Manufacturer
1/4 NPT Stainless Steel In-line valves	800	Manufacturer
1/4 NPT Stainless Steel Nipple	3000	ASTM A733
2 in NPT M to 1/4 NPT F Valve Adaptor	3000	ASTM A105
1/4 in NPT Pressure Sensors	400, 0 - 200 meas. range	Manufacturer
1/4 in NPT Bung Plug	300	ASTM A351

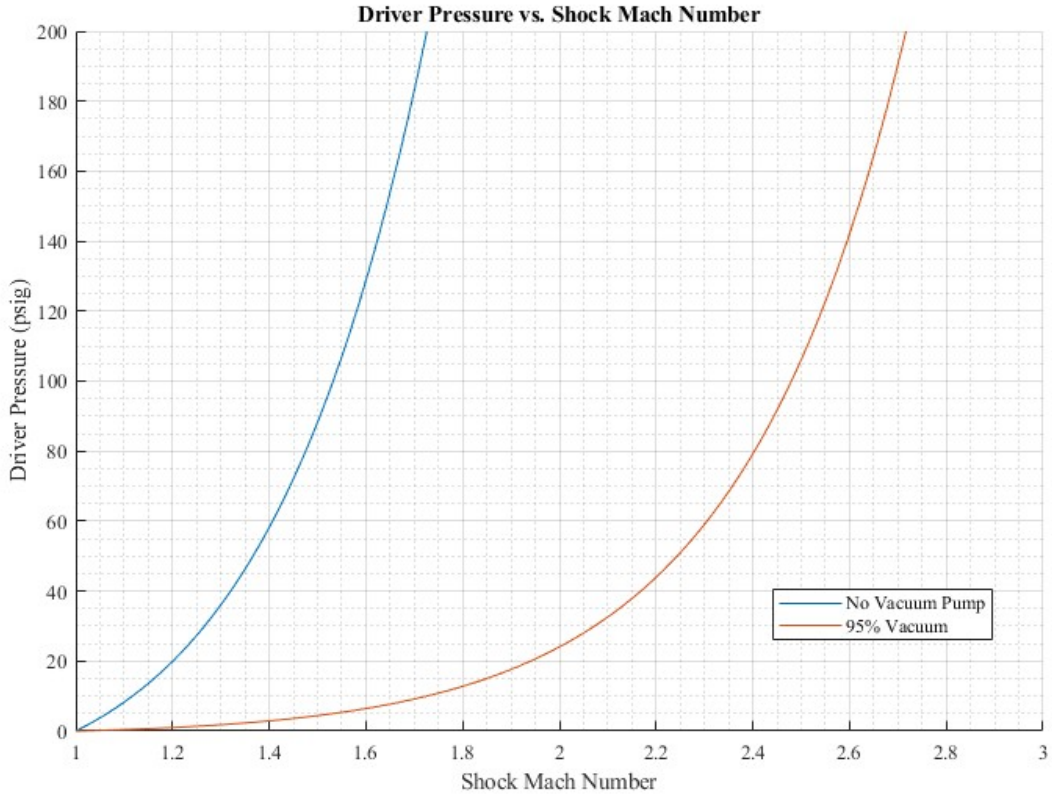
**Table 1 Maximum Working Pressures of all piping components**

Table 1 lists the maximum working pressures of all piping components used in the assembly. In the Shock Tube's current AE315 lab configuration, the design pressure was limited by the SWT pressure regulator which supplies up to 160 psig. All piping components' maximum pressure ratings exceed this limit. The only exception is the vacuum gauge; however, the inline valve should be closed after vacuuming is complete, isolating that component from the shockwave overpressure. If the hose, quick disconnects, and driver transducer were replaced with higher rated components, the system could probably be operated up to 600 psi, where the flange seal rating begins to become the limiting factor.

Using the shock tube relation, equation 1, the theoretical maximum incident Mach numbers can be plotted vs. driver pressure [1]. The theory suggests maximum Mach numbers of approximately 1.6 and 2.6 are achievable for a ambient and vacuumed driven section. A comparison between the theoretical and actual performance is shown in the testing

results section. It should be noted that an error was made in the proposal which exaggerated the achievable Mach numbers and should not be used as a reference.

$$\frac{p_4}{p_1} = \frac{1 + \frac{2\gamma_1}{\gamma_1+1}(M_s^2 - 1)}{\left[1 - \frac{\gamma_4-1}{\gamma_1-1} \frac{a_1}{a_4} \left(\frac{M_s^2-1}{M_s}\right)\right]^{\frac{2\gamma_4}{\gamma_4-1}}} \quad (1)$$



**Fig. 2 Relationship between driver pressure and shock Mach number**

## E. Pressure Transducer

A pressure transducer will be integrated into the shock tube to enable time-resolved measurement of pressure during shock wave propagation. These data will be used to validate shock wave strength, monitor diaphragm performance, and compare results across test conditions.

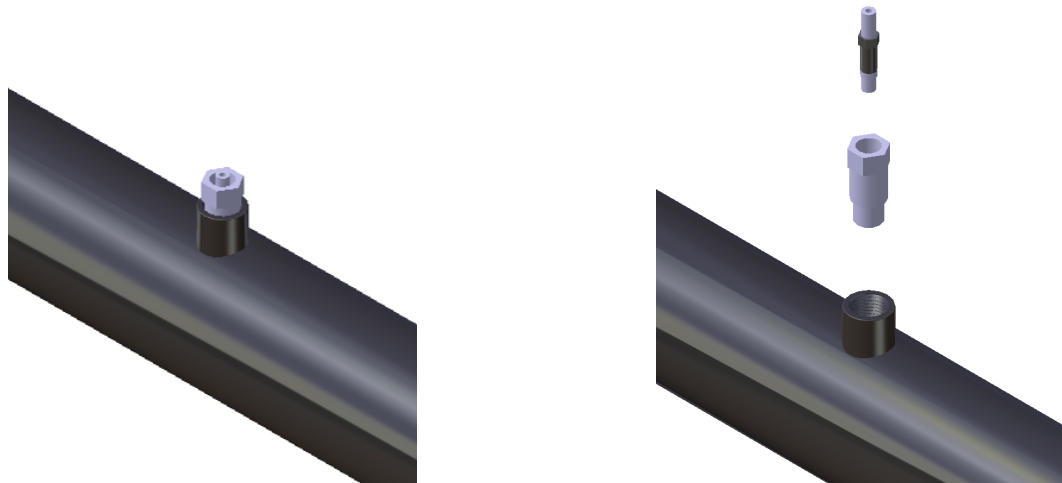
The selected transducer for reference is PCB Model 111A24 ICP® dynamic pressure sensor. It is rated for 1,000 psi with a sensitivity of 5.0 mV/psi. The sensor features a 0.218-inch Invar diaphragm, a 5/16-24 UNF-2A threaded stud, and a hermetically sealed stainless steel housing. It has a resonant frequency of 400 kHz or greater and a rise time of 1.5  $\mu$ s or less, making it suitable for capturing shock wave events. Electrical output is provided through a 10-32 coaxial jack compatible with standard ICP signal conditioning. The adapter and mounting design are based on the physical specifications of the PCB 111 Series. Alternate models from this product family can be accommodated without modification, provided they share the same thread size, sealing method, and envelope dimensions.

An off-the-shelf 1/4" NPT stainless steel bung will be welded into the wall of the driven section. The bung has a smooth outer diameter of 0.75 inches and contains a standard tapered 1/4" NPT internal thread. The shock tube's schedule 80 pipe has an outer diameter of 2.375 inches. The bung geometry was added to the CAD model to confirm fit and alignment prior to welding.



**Fig. 3 CAD of Pipe With Welded Bung, Fitted with Pressure Transducer and Adapter (Compact View)**

Figure 3 shows an assembled geometry of a cut section of the shock tube, while Figure 4 provides exploded views of the adapter and transducer to clarify individual component integration.



**(a) Transducer and Adapter (Compact View)**

**(b) Transducer and Adapter (Exploded View)**

**Fig. 4 Exploded Views of Pressure Transducer, Adapter, and Pipe Assembly**

### **Adapter Geometry and Fit-Up**

The following figures were taken directly from the technical drawing sheet used for adapter machining.

The adapter will be machined from stainless steel and features a 1/4" NPT male thread to interface with the welded bung. The sensor side includes a 5/16-24 UNF-2B internal thread and a counterbore to seat the sensor flush with the inner pipe wall. The adapter was modeled in a generously seated position (over-torqued) to ensure no material intrudes into the shock tube. This conservative condition accounts for uncertainty in NPT thread engagement and guarantees a clean internal profile.



**Fig. 5 Isometric View of Adapter from Drawing Sheet**

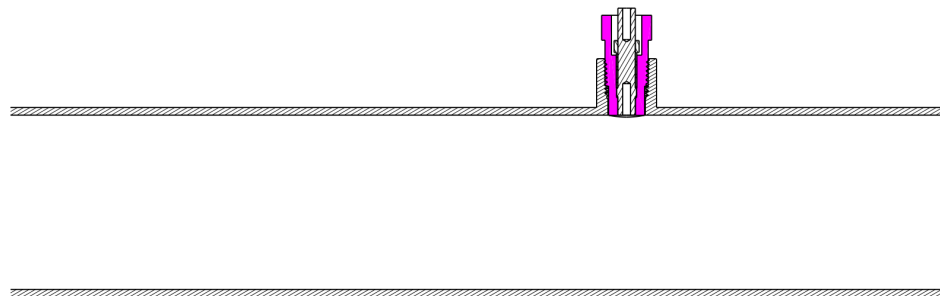


**Fig. 6 Cross-Section Showing Adapter Fit-Up and Engagement Depth**

The sensor will be connected to the data acquisition system using a shielded coaxial cable and a BNC bulkhead connector (Amphenol 31-5431-10 or equivalent). Integration will occur after all components are tested and confirmed to be sealed.

## F. Test-section Design

The design of the test-section included geometry selection, material selection, sealing (Garlock technical manual or elastomers) and attachment to shock tube, and lastly FEA. Based on the literature review from the proposal, three common designs for shock tubes with see-through optical access exist: square to circular transition, constant circular cross-section, and decreased circular cross-section. Ultimately, a mix between the last two was chosen due to the manufacturing difficulties of a transition section: the test-section has a constant circular cross-section with a gap between the end of the pipe thread and the beginning of the test-section. A picture of the CAD is shown in figure 7. The geometry provides a 6.88 inch extension from the end of the shock tube, with a 3.75 in long window on either side. The back of the test-section is flush with the end of the window to allow for easier application and testing of PSP.

The test-section is secured to the Schedule 80 pipe using 2 in NPT threads. As a result, it was safest to manufacture the test-section out of a material with similar shear strength to 304/304L. In this case 1018 carbon steel was chosen as it was the most cost effective option. The threads were specified per ASME B1.20.1 and thus should theoretically hold a reliable seal up to 3,900 psig, when properly tightened with thread sealant applied. The window inserts were sealed with a Durometer 60A neoprene gasket that covers the bottom surface of the bolted plates, sealing the gap between the acrylic window surface and the frame. No sealing pressure information was provided by the manufacturer; however, based on Garlock's gasketing technical manual, Durometer 60A elastomeric gaskets should seal to 250 psig when a 600 psi contact stress is applied to the gasket by tightening the bolts. This pressure rating is sufficient for the AE315 lab configuration.

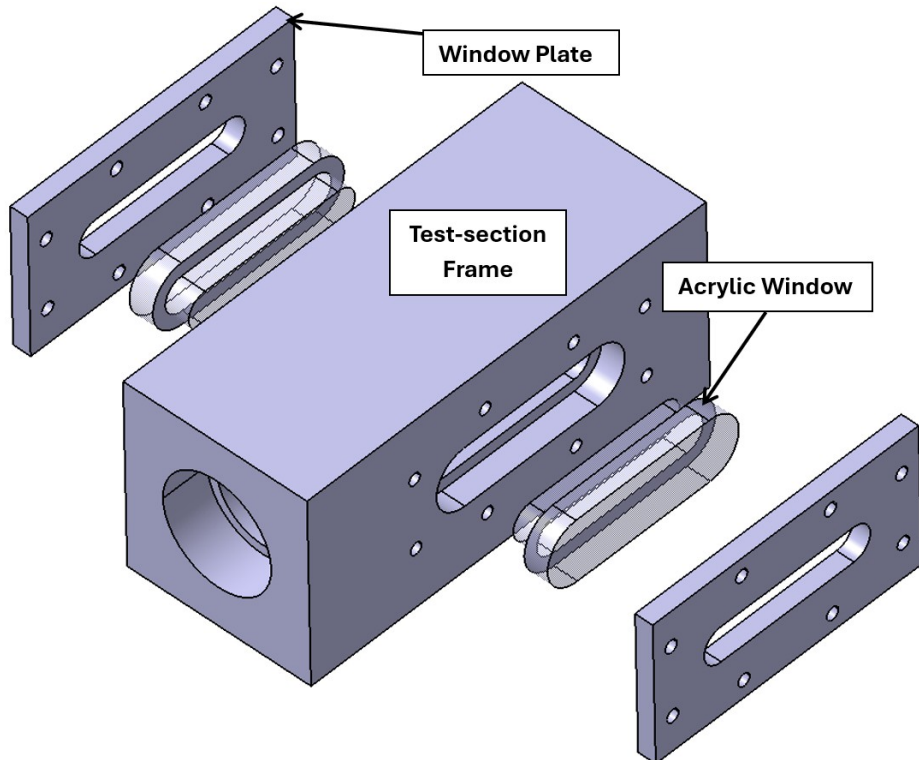


**Fig. 7 CAD of Test-section assembly**

Lastly, an FEA analysis was conducted on the test-section assembly to verify its structural integrity under a design loading of 600 psig internal pressure. For the most conservative result, the supporting structure of the pipe was omitted and the chamber was constrained such that it could freely deform axially about the circular channel under the loading. An additional frictionless support was added to the front face to prevent translational motion. A bonded contact was used between the window plates and frame due to the use of pre loaded bolts, while a rough (frictional) contact that allowed separation was used between the window and the frame.

Figure 8 shows the equivalent stress plotted on the model. The maximum occurs at the edge of the window frame cutout, with a value of 3713.4 psi, corresponding to a minimum factor of safety against yeilding of about 14 for 1018

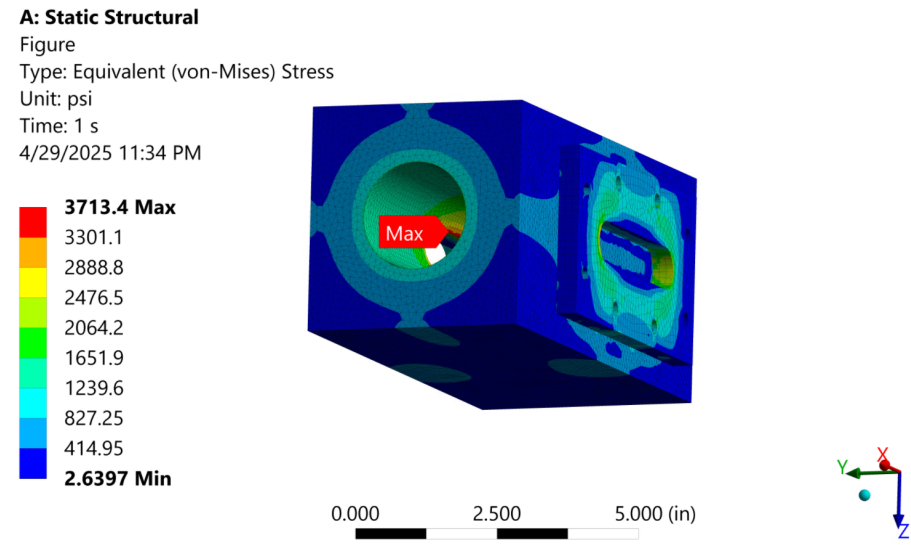


**Fig. 8 CAD of Test-section assembly**

Steel.

## IV. Testing

### A. Standard Operating Procedure

The following outlines the basic operating procedure for the refurbished shock tube. More steps will need to be added as machining for the test section is completed and pressure transducers are installed.

#### System Preparation

- 1) **Pressurize the Air Tank:** Activate the air compressor and allow the high-pressure air tank to reach a target pressure of 160 psi. Monitor the pressure gauge to ensure the desired level is achieved.
- 2) **Prepare the Schlieren System:** Carefully position the schlieren imaging system in alignment with the shock tube's exit section. Adjust the optical components (light source, lenses, knife edge) to obtain a focused and sensitive field of view for visualizing the shock wave phenomena. Initiate a system check to confirm proper functionality.
- 3) **Fabricate Diaphragms:** Using provided templates or specifications, cut Mylar sheets to the precise dimensions required for the shock tube's diaphragm interface. Ensure clean, burr-free edges to promote consistent and reliable rupture.
- 4) **Assemble the Shock Tube:** Align and reattach the driver section to the driven section of the shock tube. Carefully place a newly fabricated Mylar diaphragm between the connecting flanges, ensuring proper seating and alignment. Securely fasten the driver and driven sections using the appropriate bolts or clamps, ensuring an airtight seal.
- 5) **Install Instrumentation:** Connect the pressure transducer to the designated port on the shock tube. Ensure the transducer is securely attached and properly calibrated according to manufacturer specifications. Verify the data acquisition system connected to the transducer is operational and ready to record pressure-time history.

#### Experiment Initiation

- 1) **Initiate Recording:** Start the schlieren imaging system to commence data acquisition. Verify that the recording parameters (frame rate, duration, etc.) are set according to the experimental requirements.
- 2) **Trigger the Shock:** Activate the trigger mechanism to rapidly release the pressurized air from the storage tank

into the driver section of the shock tube. This sudden pressure increase will cause the Mylar diaphragm to rupture, generating a shock wave that propagates down the driven section.

### Data Acquisition

- Observe and Record:** The schlieren imaging system will capture the visual propagation of the shock wave and any subsequent flow phenomena exiting the shock tube. Simultaneously, the pressure transducer will record the pressure-time history at its installed location. Ensure continuous monitoring of both systems throughout the experiment.

### B. Testing Configuration

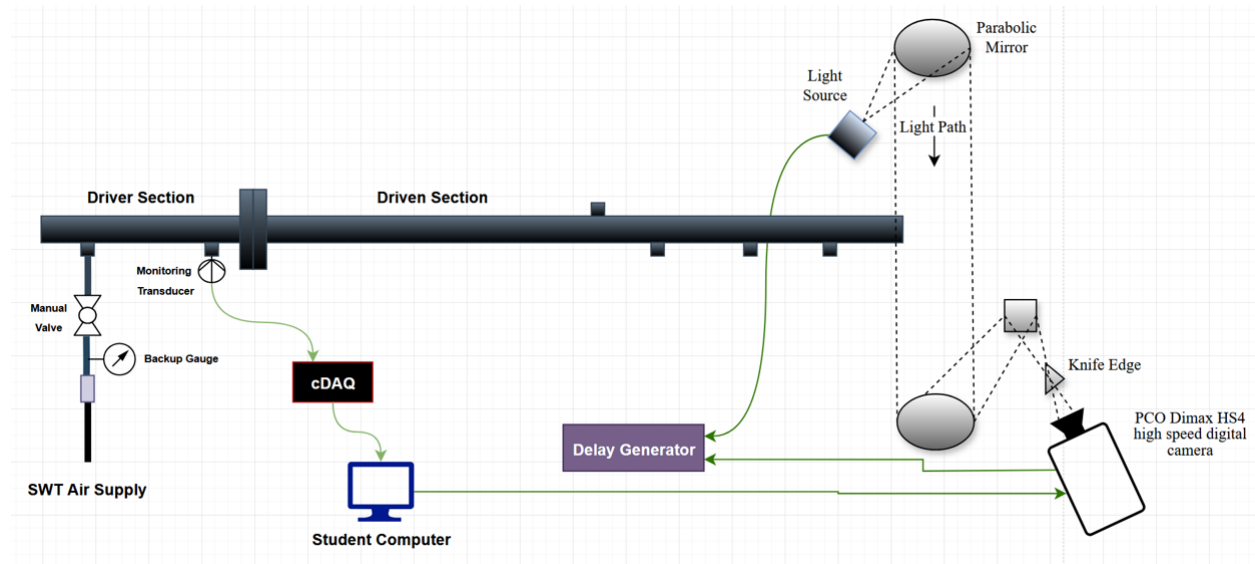


**Fig. 9 Schematic of shock tube during testing**

Figure 9 shows a overview of the test setup including the shock tube itself, pressure monitoring, and schlieren imaging equipment. The shock tube can be operated with both the shop air available in most labs or the larger compressor and storage tank found in LB182B. Pressure monitoring in the driver section is achieved using a 0-200 psig pressure transducer connected to a national instruments data acquisition device. A Z-type schlieren imaging setup is used at the exit of the shock tube to visualize the shockwave and density gradients produced when fired.

### C. Results

The open ended shock tube was tested at multiple driver pressures ranging from approximately 7 psig to 162 psig. Eight runs were conducted with varying diaphragm thicknesses in the range of 0.0002 to 0.005 inches. Figure 10 shows the driver section pressure over time for each test as it was filled to the point of diaphragm rupture. Although the majority of the tests ended in the shock tube firing, run 4 and 5 shown in plots d and e failed to reach the diaphragm burst pressure. Figure 11 shows a comparison between the theoretical burst pressure for a mylar diaphragm taken from the Air Force Flight Dynamics Laboratory Stress Manual [2] and the experimental results for a variety of diaphragm thicknesses. Comparing the two shows the experimental results to align well with the theoretical values however slightly higher pressures than predicted are required with thicker diaphragms. This could be due to the diaphragm deforming the gasket material enough to provide some relief from the stresses caused by the pressure imbalance or simply due to unforeseen effects of stacking diaphragms. By conducting these experiments, the data is able to be extrapolated allowing for burst pressure predictions of untested diaphragm thicknesses.

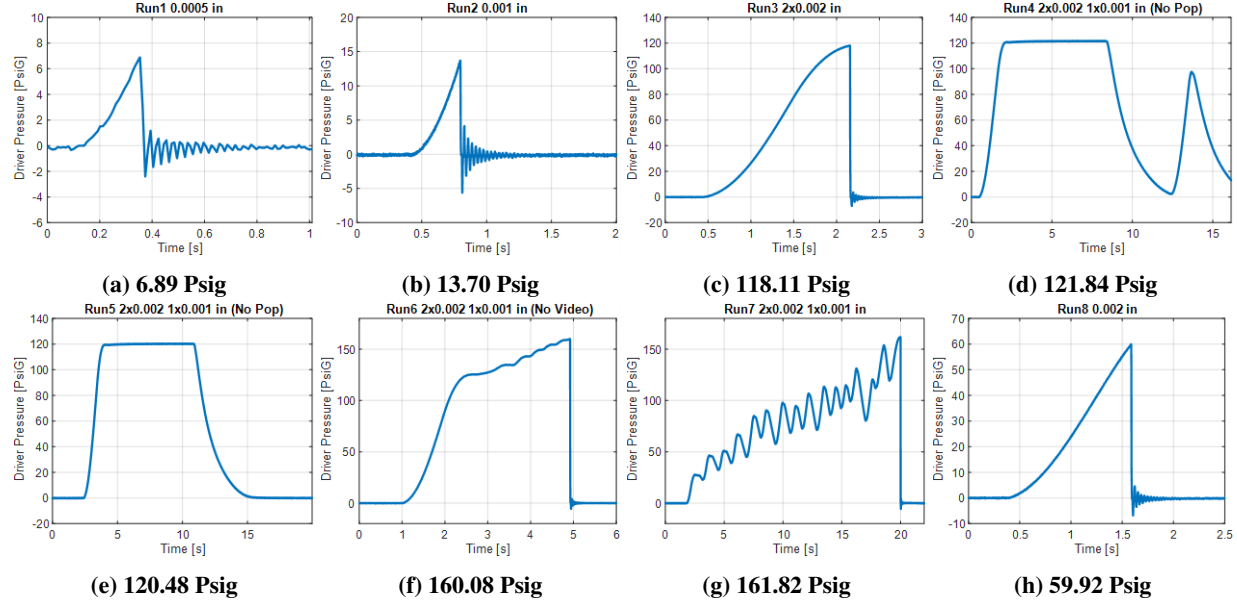


**Fig. 10** Driver section pressure and corresponding diaphragm burst pressure.

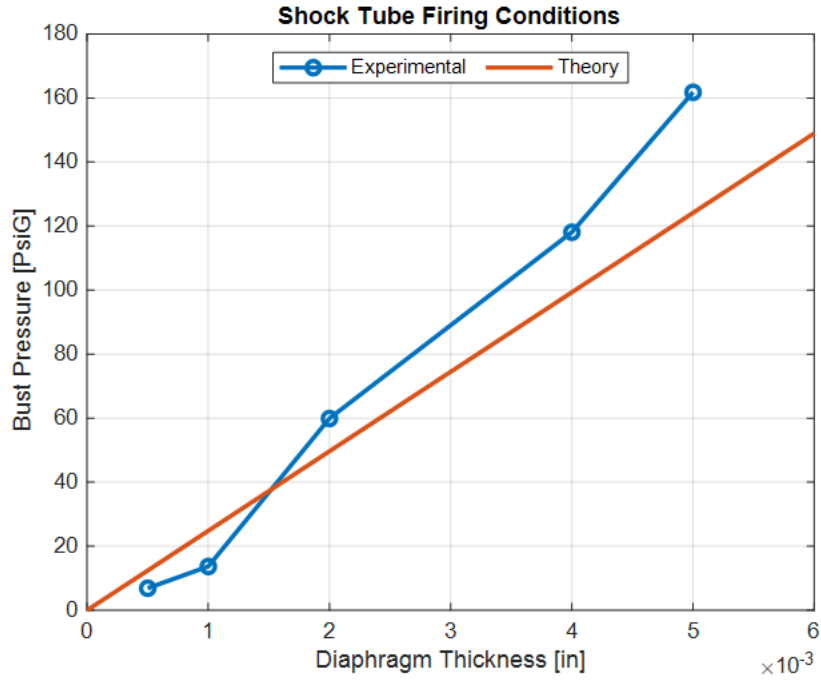


**Fig. 11** Diaphragm burst pressure determined experimentally compared to the theoretical value.

High-speed schlieren imaging was used to capture shock propagation at 50,000 frames per second. A sample image sequence from Run 3 is shown in Figure 12 with every 10th frame displayed for an effective inter-frame time of 0.002 seconds. This test was performed with a moderate driver pressure of 118 psig through the use of two stacked 0.002 inch thick diaphragms. The sequence shows a well defined initial shockwave followed by a vortex ring structure that propagates through the field of view. After the vortex ring has passed, supersonic flow is observed with shock structures indicating under-expanded conditions. These shock structures are not present in tests where the driver section was pressurized to less than 60 psig meaning the cutoff for achieving supersonic flow at the exit is between 30 and 60 psig.

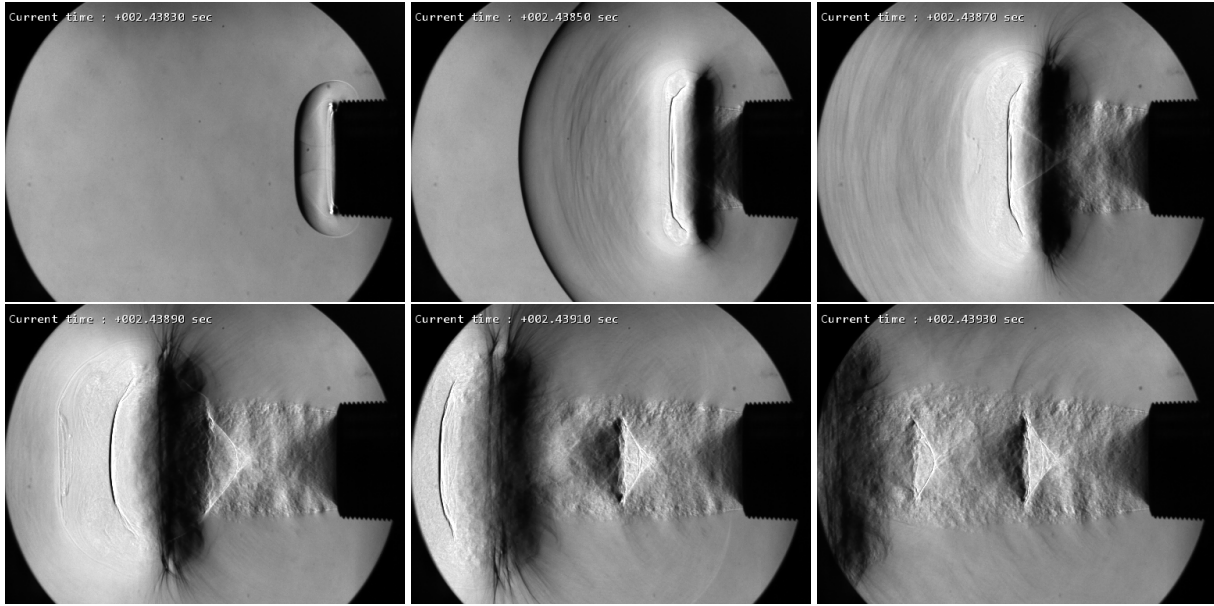


**Fig. 12** Image sequence of run 3. Video captured at 50,000 fps with every 10th image shown.

To calculate an approximate shockwave Mach number, two consecutive schlieren frames were taken from the first moment the shock is visible in each run. The distance in pixels from the exit of the tube to the shock itself was measured using ImageJ and the difference was found to establish how many pixels the shock moves in one frame of video. To convert these distances from pixels to inches, the 2 inch NPT threads with a pitch of 11.5 threads per inch was used as a scale. A visual example of this process is shown in figure 13 with results plotted against the theoretical shockwave Mach numbers in figure 14. The comparison shows that the shock tube produces shocks with Mach numbers slightly lower than that predicted by theory however the general trend and shape of the curve compares well. This could be due to viscous effects dissipating energy as the shock travels down the driven section or energy being used in the act of deforming and busting the diaphragm.

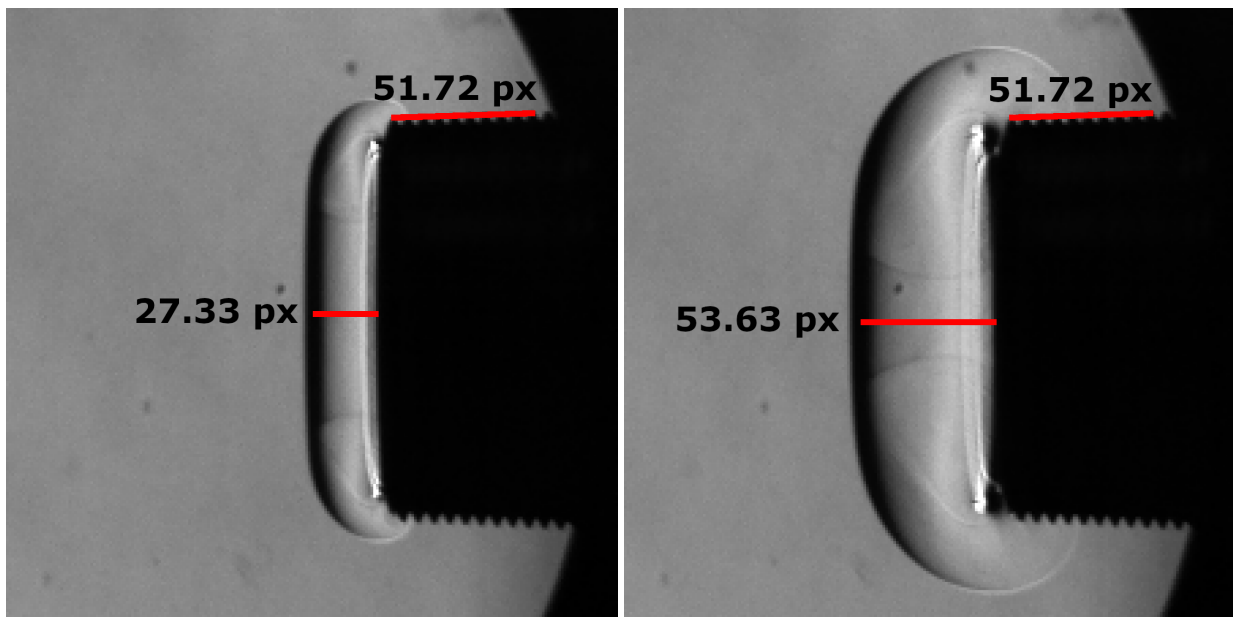


**Fig. 13** Example of position measurement used to determine the shockwave Mach number.

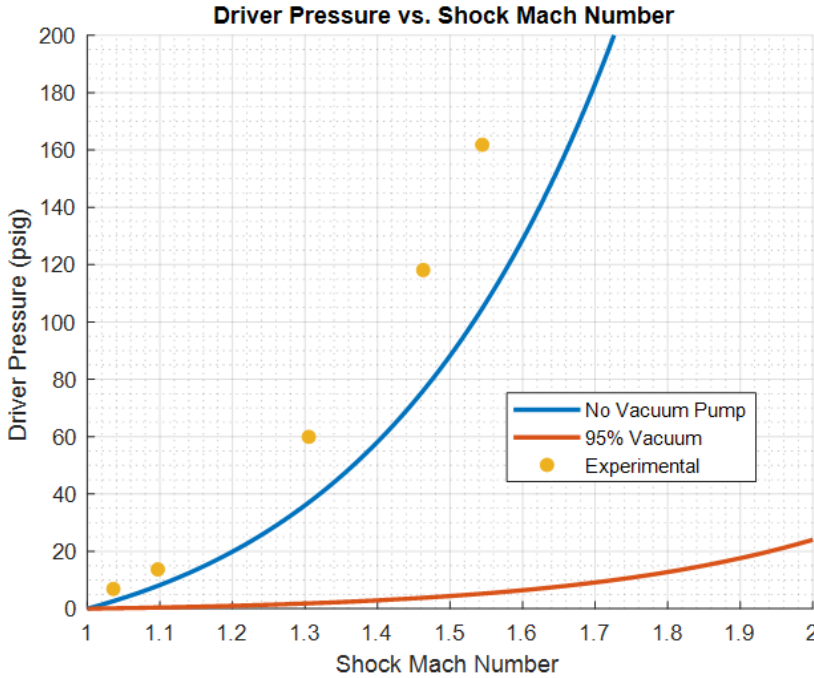


**Fig. 14 Shockwave Mach number determined experimentally compared to the theoretical value.**

## V. Lessons Learned and Future Work

During preliminary testing, several challenges were identified that will be addressed to improve experimentation in the future. Limited testing space and a lack of key tools hindered our testing and led us to delayed or even rescheduled testing sessions, highlighting the importance of complete plan for experimentation. Also, it was observed that using pre-cut diaphragms or a diaphragm press could streamline setup and increase the amount of tests performed in a certain amount of time. The process of securing and removing nuts also proved tedious with manual tools, prompting a need for an electric drill for increased speed and ease. Lastly, it became clear that the pressure regulator should be tested independently before integration, to avoid delays or inaccuracies during full system trials.

The upcoming phase of the project will focus on completing assembly of the test section as well as further testing. This includes the manufacture of pressure taps and the assembly of the test section, both of which are critical components for accurate data collection. Also, a lab procedure written for the AE 315 lab will be completed to ensure the shock tube can be properly utilized for experimentation and learning. Additionally, a comprehensive Standard Operating Procedure (SOP) will be written to ensure safety and repeatability in all testing and use of the shock tube.

## **References**

- [1] Anderson, D., J, *Modern Compressible Flow with Historical Perspective*, 4<sup>th</sup> ed., McGraw-Hill, New York, 2021, Chap. 7.
- [2] Maddux, V. L. A. G. J. F., G. E., and Morritz, T., “Stress Analysis Manual,” Tech. rep., Technology Inc, Dayton OH, 1969.